Antiviral efficacy of the SARS-CoV-2 XBB breakthrough infection sera against Omicron subvariants including EG.5

Yu Kaku[1#], Yusuke Kosugi[1,2#], Keiya Uriu[1,2#], Jumpei Ito[1,3#], Jin Kuramochi[4,5], Kenji Sadamasu[6], Kazuhisa Yoshimura[6], Hiroyuki Asakura[6], Mami Nagashima[6], The Genotype to Phenotype Japan (G2P-Japan) Consortium, Kei Sato[1,2,3,7,8,9,10*]

[1] Division of Systems Virology, Department of Microbiology and Immunology, The Institute of Medical Science, The University of Tokyo, Tokyo, Japan
[2] Graduate School of Medicine, The University of Tokyo, Tokyo, Japan
[3] International Research Center for Infectious Diseases, The Institute of Medical Science, The University of Tokyo, Tokyo, Japan
[4] Interpark Kuramochi Clinic, Utsunomiya, Japan
[5] Department of Global Health Promotion, Tokyo Medical and Dental University, Tokyo, Japan
[6] Tokyo Metropolitan Institute of Public Health, Tokyo, Japan
[7] Graduate School of Frontier Sciences, The University of Tokyo, Kashiwa, Japan
[8] International Vaccine Design Center, The Institute of Medical Science, The University of Tokyo, Tokyo, Japan
[9] Collaboration Unit for Infection, Joint Research Center for Human Retrovirus infection, Kumamoto University, Kumamoto, Japan
[10] CREST, Japan Science and Technology Agency, Kawaguchi, Japan
[#] Contributed equally to this study.
*Correspondence: KeiSato@g.ecc.u-tokyo.ac.jp (Kei Sato)

Conflict of interest: The authors declare that no competing interests exist.
Word count: 400/500 words, 6/8 references

Abstract

As of July 2023, EG.5.1 (a.k.a. XBB.1.9.2.5.1), a XBB subvariant bearing the S:Q52H and S:F456L substitutions, alongside the S:F486P substitution (Figure S1A), has rapidly spread in some countries. On July 19, 2023, the WHO classified EG.5 as a variant under monitoring. First, we showed that EG.5.1 exhibits a higher effective reproduction number compared with XBB.1.5, XBB.1.16, and its parental lineage (XBB.1.9.2), suggesting that EG.5.1 will spread globally and outcompete these XBB subvariants in the near future. We then addressed whether EG.5.1 evades from the antiviral effect of the humoral immunity induced by breakthrough infection (BTI) of XBB subvariants and performed a neutralization assay using XBB BTI sera. However, the 50% neutralization titer (NT50) of XBB BTI sera against EG.5.1 was comparable to those against XBB.1.5/1.9.2 and XBB.1.16. Moreover, the sensitivity of EG.5.1 to convalescent sera of XBB.1- and XBB.1.5-infected hamsters was similar to those of XBB.1.5/1.9 and XBB.1.16. These results suggest that the increased Re of EG.5.1 is attributed to neither increased infectivity nor immune evasion from XBB BTI, and the emergence and spread of EG.5 is driven by the other pressures. We previously demonstrated that Omicron BTI cannot efficiently induce antiviral humoral immunity against the variant infected. In fact, the NT50s of the BTI sera of Omicron BA.1, BA.2, and BA.5 against the variant infected were 3.0-, 2.2-, and 3.4-fold lower than that against the ancestral B.1.1 variant, respectively. However, strikingly, we found that the NT50 of the BTI sera of XBB1.5/1.9 and XBB.1.16 against the variant infected were 8.7- and 8.3-fold lower than that against the B.1.1 variant. These results suggest that XBB BTI cannot efficiently induce antiviral humoral immunity against XBB subvariants.

Text

The SARS-CoV-2 XBB lineage is a recombinant Omicron lineage that emerged in the summer of 2022[1]. As of July 2023, the XBB sublineages, most notably those bearing the F486P substitution in the spike protein (S; S:F486P), such as XBB.1.5 and XBB.1.16, have rapidly spread and become predominant in the world (https://nextstrain.org/). As of July 2023, EG.5.1 (a.k.a. XBB.1.9.2.5.1), a XBB subvariant bearing the S:Q52H and S:F456L substitutions, alongside the S:F486P substitution (**Figure S1A**), has rapidly spread in some Asian and North American countries (**Figures S1B**). On July 19, 2023, the WHO classified EG.5 as a variant under monitoring.[2] In fact, our analyses showed that EG.5.1 exhibits a higher effective reproduction number (R_e) compared with XBB.1.5, XBB.1.16, and its parental lineage (XBB.1.9.2), suggesting that EG.5.1 will spread globally and outcompete these XBB subvariants in the near future (**Figure S1C**).

To assess the possibility that the enhanced infectivity of EG.5.1 contributes to its augmented R_e, we prepared pseudoviruses with the S proteins of EG.5.1, XBB.1.5/1.9.2, and their derivatives. However, both S:Q52H and S:F456L did not increase pseudovirus infectivity, and the pseudovirus infectivity of EG.5.1 was significantly lower than that of its parental lineage (XBB.1.9.2) (**Figure S1D**). We then addressed whether EG.5.1 evades the antiviral effect of the humoral immunity induced by breakthrough infection (BTI) of XBB subvariants and performed a neutralization assay using XBB BTI sera. However, the 50% neutralization titer (NT_{50}) of XBB BTI sera against EG.5.1 was comparable to those against XBB.1.5/1.9.2 and XBB.1.16 (**Figure S1E**). Moreover, the sensitivity of EG.5.1 to convalescent sera of XBB.1- and XBB.1.5-infected hamsters was similar to those of XBB.1.5/1.9 and XBB.1.16 (**Figure S1F**). These results suggest that the increased R_e of EG.5.1 is attributed to neither increased infectivity nor immune evasion from XBB BTI, and the emergence and spread of EG.5 is driven by the other pressures.

We previously demonstrated that Omicron BTI cannot efficiently induce antiviral humoral immunity against the variant infected.[1,3-6] In fact, the NT_{50}s of the BTI sera of Omicron BA.1, BA.2, and BA.5 against the variant infected were 3.0-, 2.2-, and 3.4-fold lower than that against the ancestral B.1.1 variant, respectively (**Figure S1G**). Strikingly, however, we found that the NT_{50} of the BTI sera of XBB1.5/1.9.2 and XBB.1.16 against the variant infected were 8.7- and 8.3-fold lower than that against the B.1.1 variant (**Figure S1E**). These results suggest that XBB BTI cannot efficiently induce antiviral humoral immunity against XBB subvariants.

Grants

Supported in part by AMED SCARDA Japan Initiative for World-leading Vaccine Research and Development Centers "UTOPIA" (JP223fa627001, to Kei Sato), AMED SCARDA Program on R&D of new generation vaccine including new modality application (JP223fa727002, to Kei Sato); AMED Research Program on Emerging and Re-emerging Infectious Diseases (JP22fk0108146, to Kei Sato; JP21fk0108494 to G2P-Japan Consortium and Kei Sato; JP21fk0108425, to Kei Sato; JP21fk0108432, to Kei Sato; JP22fk0108511, to G2P-Japan Consortium and Kei Sato; JP22fk0108516, to Kei Sato; JP22fk0108506, to Kei Sato); AMED Research Program on HIV/AIDS (JP22fk0410039, to Kei Sato); JST PRESTO (JPMJPR22R1, to Jumpei Ito); JST CREST (JPMJCR20H4, to Kei Sato); JSPS KAKENHI Grant-in-Aid for Early-Career Scientists (23K14526, to Jumpei Ito); JSPS Core-to-Core Program (A. Advanced Research Networks) (JPJSCCA20190008, Kei Sato); JSPS Research Fellow DC2 (22J11578, to Keiya Uriu); JSPS Research Fellow DC1 (23KJ0710, to Yusuke Kosugi); The Tokyo Biochemical Research Foundation (to Kei Sato); The Mitsubishi Foundation (to Kei Sato).

Declaration of interest

J.I. has consulting fees and honoraria for lectures from Takeda Pharmaceutical Co. Ltd. K.S. has consulting fees from Moderna Japan Co., Ltd. and Takeda Pharmaceutical Co. Ltd. and honoraria for lectures from Gilead Sciences, Inc., Moderna Japan Co., Ltd., and Shionogi & Co., Ltd. The other authors declare no competing interests. All authors have submitted the ICMJE Form for Disclosure of Potential Conflicts of Interest. Conflicts that the editors consider relevant to the content of the manuscript have been disclosed.

116 **References**

117 1. Tamura T, Ito J, Uriu K, et al. Virological characteristics of the SARS-CoV-
118 2 XBB variant derived from recombination of two Omicron subvariants. *Nat*
119 *Commun* 2023; **14**(1): 2800.
120 2. WHO. "Tracking SARS-CoV-2 variants (July 19, 2023)"
121 https://www.who.int/en/activities/tracking-SARS-CoV-2-variants. 2023.
122 3. Yamasoba D, Kimura I, Nasser H, et al. Virological characteristics of the
123 SARS-CoV-2 Omicron BA.2 spike. *Cell* 2022; **185**(12): 2103-15.e19.
124 4. Ito J, Suzuki R, Uriu K, et al. Convergent evolution of the SARS-CoV-2
125 Omicron subvariants leading to the emergence of BQ.1.1 variant. *Nat Commun*
126 2023; **14**(1): 2671.
127 5. Uriu K, Ito J, Zahradnik J, et al. Enhanced transmissibility, infectivity, and
128 immune resistance of the SARS-CoV-2 omicron XBB.1.5 variant. *Lancet Infect*
129 *Dis* 2023; **23**(3): 280-1.
130 6. Yamasoba D, Uriu K, Plianchaisuk A, et al. Virological characteristics of
131 the SARS-CoV-2 omicron XBB.1.16 variant. *Lancet Infect Dis* 2023; **23**(6): 655-
132 6.
133

Supplementary Appendix

Table of Contents

Supplementary Discussion

On June 15, 2023, the FDA's Vaccines and Related Biological Products Advisory Committee issued a recommendation for the use of the monovalent XBB.1.5 vaccine for the purpose of booster vaccination in the autumn of 2023.[7] Because booster vaccination with XBB.1.5-containing vaccines induces >10-fold anti-XBB neutralizing antibodies,[8] the monovalent XBB.1.5 vaccine may potentially induce anti-XBB humoral immunity. However, here we showed that the immunogenicity of XBB subvariants is lower than that of previous Omicron subvariants (**Figure S1E and S1G**). Therefore, the immune activation induced by XBB BTI and further XBB vaccination may be less effective than expected. It should be noted that our results presented here do not imply ineffectiveness of XBB-containing vaccines; however, our data suggest that XBB BTI does not sufficiently induce anti-XBB humoral immunity.

Materials and Methods

Ethics statement

All protocols involving specimens from human subjects recruited at Interpark Kuramochi Clinic was reviewed and approved by the Institutional Review Board of Interpark Kuramochi Clinic (approval ID: G2021-004). All human subjects provided written informed consent. All protocols for the use of human specimens were reviewed and approved by the Institutional Review Boards of The Institute of Medical Science, The University of Tokyo (approval IDs: 2021-1-0416 and 2021-18-0617).

Human serum collection

Convalescent sera were collected from fully vaccinated individuals who had been infected with BA.1 (thirteen 2-dose vaccinated; time interval between the last vaccination and infection, 71–251 days; 7–27 days after testing. n=13; average age: 43 years, range: 20–65 years, 46.2% male) (**Figure S1G**), BA.2 (nine 2-dose vaccinated and four 3-dose vaccinated; time interval between the last vaccination and infection, 4–299 days; 11–61 days after testing. n=13 in total; average age: 45 years, range: 24–82 years, 62% male) (**Figure S1G**), BA.5 (one 2-dose vaccinated, thirteen 3-dose vaccinated and one 4-dose vaccinated; time interval between the last vaccination and infection, 66–310 days; 10–23 days after testing. n=15 in total; average age: 55 years, range: 25–73 years, 47% male) (**Figure S1G**), and XBB sublineages [XBB.1.5 (one 3-dose vaccinated; time interval between the last vaccination and infection, 413 days; 38 days after testing. n=1 in total; average age: 55 years, range: 55 years, 100% male), XBB.1.9 (one 3-dose vaccinated, one 4-dose vaccinated and one 5-dose vaccinated; time interval between the last vaccination and infection, 176–246 days; 6–18 days after testing. n=3 in total; average age: 53.7 years, range: 32–88 years, 33.3% male), and XBB.1.16 (one 2-dose vaccinated, two 3-dose vaccinated and one 4-dose vaccinated; time interval between the last vaccination and infection, 223–569 days; 7–15 days after testing. n=4 in total; average age: 38.8 years, range: 18–65 years, 100% male)] (**Figure S1E**). The SARS-CoV-2 variants were identified as previously described.[1-3] Sera were inactivated at 56°C for 30 minutes and stored at –80°C until use. The details of the convalescent sera are summarized in **Table S1**.

Hamster serum collection

Animal experiments were performed as previously described.[1-14] Briefly, 4-week male Syrian hamsters purchased from Japan SLC Inc. (Shizuoka, Japan) were inoculated with 10,000 50% tissue culture infectious dose ($TCID_{50}$) of XBB.1 or XBB.1.5 via the intranasal route under anesthesia. The anesthetics used for viral infection were injected into muscles as a mixture of 0.15 mg/kg medetomidine hydrochloride (Domitor®, Nippon Zenyaku Kogyo), 2.0 mg/kg midazolam (Dormicum®, Fujifilm Wako, Cat# 135-13791) and 2.5 mg/kg butorphanol

(Vetorphale®, Meiji Seika Pharma) or 0.15 mg/kg medetomidine hydrochloride, 4.0 mg/kg alphaxaone (Alfaxan®, Jurox) and 2.5 mg/kg butorphanol at 16 days postinfection.

Epidemic dynamics analysis

In the present study, we analyzed the viral genomic surveillance data deposited in the GISAID database (https://www.gisaid.org/; downloaded on July 13, 2023). We used the data from April 1, 2023 in this analysis. We excluded the sequence records with the following features: i) a lack of collection date information; ii) sampling in animals other than humans; iii) sampling by quarantine; iv) without the PANGO lineage information; and v) having >2% undetermined (N) nucleotide sequences. In the downstream analysis, we only used sequences for PANGO lineages with >50 sequences in the dataset. We modeled the epidemic dynamics of viral lineages in six countries (China, South Korea, USA, Japan, Singapore, and Canada), where >50 sequences of XBB.1.5, XBB.1.16, and EG.5.1 were detected. We counted the daily frequency of each viral lineage. Subsequently, epidemic dynamics and relative R_e value for each viral lineage were estimated according to the Bayesian multinomial logistic model, described in our previous study.[2] Briefly, we estimated the logistic slope parameter β_l for each viral lineage using the model and then calculated relative R_e for each lineage r_l as $r_l = exp(\gamma\beta_l)$ where γ is the average viral generation time (2.1 days) (http://sonorouschocolate.com/covid19/index.php?title=Estimating_Generation_Time_Of_Omicron). For parameter estimation, the intercept and slope parameters of XBB.1.5 were fixed at 0. Consequently, the relative R_e of XBB.1.5 was fixed at 1, and those of the other lineages were estimated relative to that of XBB.1. Parameter estimation was performed via the MCMC approach implemented in CmdStan v2.31.0 (https://mc-stan.org) with CmdStanr v0.5.3 (https://mc-stan.org/cmdstanr/). Four independent MCMC chains were run with 1,000 and 4,000 steps in the warmup and sampling iterations, respectively. We confirmed that all estimated parameters showed <1.05 R-hat convergence diagnostic values and >200 effective sampling size values, indicating that the MCMC runs were successfully convergent. Information on the estimated parameters is summarized in **Table S2**. In **Figures S1B and S1C**, results for XBB.1.5, XBB.1.9.2, XBB.1.16, and EG.5.1 are shown.

Plasmid construction

Plasmids expressing the SARS-CoV-2 spike proteins of the ancestral B.1.1 (D614G-bearing virus), Omicron BA.1, BA.2, BA.5, BQ.1.1, XBB.1, XBB.1.5/1.9.2 and XBB.1.16 were prepared in our previous studies.[1,2,4,15-19] Note that the S proteins of XBB.1.5 and XBB.1.9.2 are identical (**Figure S1A**). Plasmids expressing the spike protein of EG.5.1 and its derivative were generated by site-directed overlap extension PCR using pC-SARS2-S XBB.1.5[18] as the template and the primers listed in **Table S3**. The resulting PCR fragment was subcloned into the KpnI-NotI site of the pCAGGS vector[20] using In-Fusion HD Cloning Kit (Takara, Cat# Z9650N). Nucleotide

sequences were determined by DNA sequencing services (Eurofins), and the sequence data were analyzed by SnapGene software v6.1.1 (www.snapgene.com).

Cell culture

The Lenti-X 293T cell line (Takara, Cat# 632180) and HOS-ACE2/TMPRSS2 cells (kindly provided by Dr. Kenzo Tokunaga), a derivative of HOS cells (a human osteosarcoma cell line; ATCC CRL-1543) stably expressing human ACE2 and TMPRSS2,[7,21] were maintained in Dulbecco's modified Eagle's medium (DMEM) (high glucose) (Wako, Cat# 044- 29765) containing 10% fetal bovine serum (Sigma-Aldrich Cat# 172012-500ML), 100 units penicillin and 100 ug/ml streptomycin (Sigma-Aldrich, Cat# P4333-100ML).

Pseudovirus preparation

Pseudoviruses were prepared as previously described.[1-5,7-11,13,15-19,22] Briefly, lentivirus (HIV-1)-based, luciferase-expressing reporter viruses were pseudotyped with the SARS-CoV-2 spikes. HEK293T cells (2 × 10^6 cells) were cotransfected with 1 μg psPAX2-IN/HiBiT,[23] 1 μg pWPI-Luc2,[23] and 500 ng plasmids expressing parental S or its derivatives using TransIT-293 transfection reagent (Mirus, Cat# MIR2704) according to the manufacturer's protocol. Two days post transfection, the culture supernatants were harvested and centrifuged. The amount of pseudoviruses prepared was quantified by the HiBiT assay using Nano Glo HiBiT lytic detection system (Promega,Cat# N3040) as previously described.[1-5,7-11,13,15-19,22] To measure viral infectivity, the same amount of pseudoviruses (normalized to the HiBiT value, which indicates the amount of p24 HIV-1 antigen) was inoculated into HOS-ACE2/TMPRSS2 cells. At two days postinfection, the infected cells were lysed with a Bright-Glo luciferase assay system (Promega, Cat# E2620), and the luminescent signal was measured using a GloMax explorer multimode microplate reader 3500 (Promega). The pseudoviruses were stored at –80°C until use.

Neutralization assay

Neutralization assays were performed as previously described.[1-5,7,8,10,11,13,16-19] The SARS-CoV-2 spike pseudoviruses (counting ~100,000 relative light units) were incubated with serially diluted (120-fold to 87,480-fold dilution at the final concentration) heat-inactivated sera at 37°C for 1 hour. Pseudoviruses without sera were included as controls. Then, 20 μl mixture of pseudovirus and serum was added to HOS-ACE2/TMPRSS2 cells (10,000 cells/100 μl) in a 96-well white plate. Two days post infection, the infected cells were lysed with a Bright-Glo luciferase assay system (Promega, Cat# E2620), and the luminescent signal was measured using a GloMax explorer multimode microplate reader 3500 (Promega). The assay of each serum sample was performed in triplicate, and the 50% neutralization titer (NT_{50}) was calculated using Prism 9 (GraphPad Software).

Data availability

Dataset used in the epidemic dynamics analysis in this study is available from the GISAID database (https://www.gisaid.org; EPI_SET_230725pv). The GISAID supplemental tables for EPI_SET_230725pv is available in the GitHub repository (https://github.com/TheSatoLab/EG.5.1_short).

Table S1. Human sera used in this study

SARS-CoV-2 infected	Donor ID	Sex	Age	vaccine (1st vaccination)	Date of 1st vaccination (YYYY-MM-DD)	vaccine (2nd vaccination)	Date of 2nd vaccination (YYYY-MM-DD)	vaccine (3rd vaccination)	Date of 3rd vaccination (YYYY-MM-DD)	vaccine (4th vaccination)	Date of 4th vaccination (YYYY-MM-DD)	vaccine (5th vaccination)	Date of 5th vaccination (YYYY-MM-DD)	Date of test (YYYY-MM-DD)	Date of sampling (YYYY-MM-DD)	Prior infection?
BA.1	P264	Male	60	BNT162b2	2021-08-27	BNT162b2	2021-09-18							2022-01-03	2022-01-29	No
BA.1	P265	Female	57	BNT162b2	2021-10-04	BNT162b2	2021-10-25							2022-01-04	2022-01-28	No
BA.1	P274	Female	20	mRNA-1273	2021-09-11	mRNA-1273	2021-10-09							2022-01-15	2022-01-29	No
BA.1	P276	Male	44	BNT162b2	2021-08-06	BNT162b2	2021-08-22							2022-01-20	2022-01-30	No
BA.1	P279	Male	61	BNT162b2	2021-07-03	BNT162b2	2021-07-24							2022-01-18	2022-02-05	No
BA.1	P282	Male	56	BNT162b2	2021-09-18	BNT162b2	2021-10-12							2022-01-22	2022-02-06	No
BA.1	P285	Female	65	BNT162b2	2022-01-07	BNT162b2	2022-01-28							2022-01-23	2022-02-06	No
BA.1	P295	Female	41	BNT162b2	2021-08-07	BNT162b2	2021-08-28							2022-01-25	2022-02-06	No
BA.1	2112	Male	44	BNT162b2	2021-04-21	BNT162b2	2021-05-12							2022-01-18	2022-01-25	No
BA.1	1880	Female	25	BNT162b2	2021-09-09	BNT162b2	2021-09-30							2022-01-07	2022-02-03	No
BA.1	2187	Male	32	mRNA-1273	2021-07-09	mRNA-1273	2021-08-06							2022-01-20	2022-02-05	No
BA.1	2137	Female	32	mRNA-1273	2021-07-09	mRNA-1273	2021-08-06							2022-01-19	2022-02-05	No
BA.1	2550	Female	24	BNT162b2	2021-10-12	BNT162b2	2021-11-02							2022-01-25	2022-02-05	No
BA.2	P378	Male	43	BNT162b2	2021-10-10	BNT162b2	2021-10-31	BNT162b2						2022-03-28	2022-04-10	No
BA.2	P398	Male	48	BNT162b2	2021-09-18	BNT162b2	2021-10-09	BNT162b2	2022-04-09					2022-04-13	2022-04-30	No
BA.2	P407	Male	29	mRNA-1273	2021-09-13	mRNA-1273	2021/10/11	mRNA-1273						2022-05-01	2022-05-12	No
BA.2	P401	Male	35	BNT162b2	2021-09-09	BNT162b2	2021-09-30	BNT162b2						2022-04-22	2022-05-05	No
BA.2	P412	Female	82	BNT162b2	2021-06-11	BNT162b2	2021-07-09	BNT162b2						2022-05-04	2022-05-26	No
BA.2	6449	Male	43	BNT162b2	2021-08-13	BNT162b2	2021-09-11	BNT162b2						2022-04-03	2022-04-23	No
BA.2	6355	Male	50	NA	2021-04-28	NA	2021-05-19	NA	2022-01-19					2022-04-02	2022-04-20	No
BA.2	6547	Male	54	BNT162b2	2021-08-25	BNT162b2	2021-09-15	BNT162b2						2022-04-06	2022-04-22	No
BA.2	7951	Female	71	BNT162b2	2021-06-20	BNT162b2	2021-07-16	mRNA-1273	2022-02-16					2022-04-25	2022-05-12	No
BA.2	8645	Female	41	BNT162b2	2021-05-23	BNT162b2	2021-06-13	BNT162b2	2022-01-20					2022-05-07	2022-05-20	No
BA.2	8682	Female	25	BNT162b2	2021-09-03	BNT162b2	2021-09-27	BNT162b2						2022-05-08	2022-05-24	No
BA.2	5949	Male	24	mRNA-1273	2021-08-05	mRNA-1273	2021-09-02	mRNA-1273						2022-03-22	2022-05-22	No
BA.2	8796	Female	34	BNT162b2	2021-09-26	BNT162b2	2021-10-17	BNT162b2						2022-05-10	2022-06-05	No
BA.5	P427	Female	49	NA	2021-07-30	NA	2021-08-25	NA	2022-03-18					2022-07-06	2022-07-25	No
BA.5	P439	Female	73	BNT162b2	2021-06-19	BNT162b2	2021-07-20	mRNA-1273	2022-02-04					2022-07-23	2022-08-08	No
BA.5	P451	Female	55	BNT162b2	2021-04-26	BNT162b2	2021-05-20	BNT162b2	2022-01-18					2022-07-29	2022-08-12	No
BA.5	P456	Male	44	BNT162b2	2021-08-11	BNT162b2	2021-09-01	mRNA-1273	2022-03-13					2022-08-04	2022-08-14	No
BA.5	P464	Male	63	BNT162b2	2021-08-08	BNT162b2	2021-08-29	mRNA-1273	2022-04-07					2022-08-08	2022-08-19	No
BA.5	9341	Male	56	BNT162b2	2021-08-10	BNT162b2	2021-08-31	BNT162b2	2022-03-18					2022-06-12	2022-06-30	No
BA.5	9584	Male	55	BNT162b2	2021-07-14	BNT162b2	2021-08-05	BNT162b2	2022-03-22					2022-07-08	2022-07-25	No
BA.5	11318	Female	51	BNT162b2	2021-09-01	BNT162b2	2021-09-22	mRNA-1273	2022-05-19					2022-07-24	2022-08-05	No
BA.5	23S-08	Male	25	BNT162b2	2021-04-27	BNT162b2	2021-05-18	BNT162b2	2022-01-11					2022-07-23	2022-08-08	No
BA.5	10826	Male	63	BNT162b2	2021-07-27	BNT162b2	2021-08-17	BNT162b2	2022-03-04	mRNA-1273	2022-08-09			2022-07-21	2022-08-11	No
BA.5	11079	Female	65	mRNA-1273	2021-07-08	mRNA-1273	2021-08-05	mRNA-1273	2022-03-17					2022-07-23	2022-08-11	No
BA.5	14847	Female	70	BNT162b2	2021-07-13	BNT162b2	2021-08-20	mRNA-1273	2022-03-08					2022-08-13	2022-08-25	No
BA.5	13180	Female	63	BNT162b2	2021-07-16	BNT162b2	2021-08-06	mRNA-1273	2022-03-08					2022-08-04	2022-08-25	No
BA.5	12912	Male	64	mRNA-1273	2021-09-02	mRNA-1273	2021-09-30	mRNA-1273	2021-04-01					2022-08-02	2022-08-25	No
BA.5	14956	Female	33	BNT162b2	2021-09-06	BNT162b2	2021-10-07							2022-08-13	2022-08-28	No
XBB.1.5	36708	Male	55	BNT162b2	2021-08-07	BNT162b2	2021-08-27	BNT162b2	2022-04-14					2023-06-01	2023-07-09	No
XBB.1.9	P592	Female	32	NA	NA	NA	NA	BNT162b2	2022-10-26					2023-05-06	2023-05-16	No
XBB.1.9	P595	Female	88	BNT162b2	2021-05-18	BNT162b2	2021-06-08	mRNA-1273	2022-02-04	mRNA-1273	2022-07-19	bivalent, Pfizer-BioNTech	2022-11-18	2023-05-13	2023-05-19	No
XBB.1.9	KS-230718	Male	41	BNT162b2	2021-06-17	BNT162b2	2021-07-07	mRNA-1273	2022-03-28	mRNA-1273.222	2022-10-27			2023-06-30	2023-07-18	No
XBB.1.16	P601	Male	38	BNT162b2	2021-11-05	BNT162b2	2021-11-26	BNT162b2	2022-05-27					2023-07-06	2023-07-14	No
XBB.1.16	P593	Male	65	BNT162b2	2021-08-02	BNT162b2	2021-08-30	BNT162b2	2022-04-03					2023-05-09	2023-05-16	No
XBB.1.16	P594	Male	18	BNT162b2	2021-09-06	BNT162b2	2021-10-15							2023-05-07	2023-05-19	No
XBB.1.16	JI-230718	Male	34	mRNA-1273	2021-07-19	mRNA-1273	2021-08-20	mRNA-1273	2022-05-13	mRNA-1273.222	2022-11-22			2023-07-03	2023-07-18	Yes

NA, not applicable.

Table S2. Estimated relative Re and epidemic dynamics modeling parameters of the representative SARS-CoV-2 Omicron sublineages spreading

Country	PANGO lineage	Posterior mean	Posterior 2.5 percentile	Posterior 97.5 percentile	R-hat value	Effective sampling size (ESS_bulk)	Effective sampling size (ess_tail)
Canada	EG.5.1	1.194	1.156	1.235	1.000	28020.167	11760.151
Canada	XBB.1.5.10	1.130	1.098	1.163	1.000	28852.170	11060.454
Canada	XBB.1.5.77	1.129	1.099	1.160	1.000	26316.643	11847.772
Canada	FL.2	1.117	1.087	1.148	1.000	23850.488	12222.184
Canada	FL.4	1.106	1.093	1.118	1.000	21557.407	11294.275
Canada	EG.5.2	1.098	1.070	1.127	1.001	22065.019	11225.833
Canada	XBB.1.9.2	1.093	1.077	1.110	1.000	24401.962	11272.720
Canada	XBB.1.16	1.092	1.085	1.100	1.000	16188.077	12184.423
Canada	XBB.1.16.3	1.091	1.065	1.117	1.000	21908.154	12291.440
Canada	XBB.1.16.1	1.087	1.073	1.101	1.000	22902.095	11224.878
Canada	FL.5	1.077	1.061	1.095	1.000	24573.253	11876.335
Canada	EG.1	1.076	1.059	1.093	1.000	25130.931	11995.833
Canada	FE.1.1.1	1.073	1.053	1.094	1.000	24534.713	12577.649
Canada	FD.1.1	1.071	1.063	1.078	1.000	19787.553	12077.306
Canada	XBB.1.16.2	1.070	1.052	1.088	1.001	23073.775	12690.091
Canada	XBB.1.5.37	1.069	1.047	1.092	1.000	27311.861	11906.712
Canada	XBB.1.9.1	1.067	1.058	1.076	1.000	19615.125	12280.830
Canada	XBB.2.3.2	1.066	1.044	1.087	1.000	25803.316	12386.694
Canada	FL.13	1.064	1.043	1.087	1.000	26894.810	11857.820
Canada	XBB.2.3.3	1.059	1.034	1.083	1.000	22087.655	11522.770
Canada	XBB.2.3	1.046	1.029	1.063	1.001	25501.988	12326.880
Canada	XBB.1.5.62	1.039	1.010	1.068	1.001	28943.932	11380.550
Canada	XBB.1.5.15	1.034	1.013	1.054	1.000	25653.395	11745.767
Canada	XBB.1.5.4	1.026	1.002	1.049	1.000	25794.898	11808.858
Canada	XBB.1.5.13	1.023	1.008	1.038	1.001	26031.661	12118.199
Canada	XBB.1.5.49	1.014	1.000	1.027	1.000	23714.177	12657.722
Canada	XBB.1.5.17	0.999	0.979	1.019	1.000	28516.422	11615.119
Canada	CH.1.1	0.998	0.972	1.025	1.000	30231.545	12166.557
Canada	DV.1.1	0.995	0.979	1.010	1.000	25337.707	12063.520
Canada	XBB.1.5.1	0.993	0.977	1.009	1.000	23550.112	12375.932
Canada	XBB.1.5.50	0.993	0.975	1.010	1.000	29322.905	12455.737
Canada	XBB.1.5.19	0.992	0.962	1.022	1.000	27375.832	12903.215
Canada	XBB.1.5.12	0.990	0.959	1.020	1.000	25564.766	12585.821
Canada	XBB.1.5.2	0.983	0.963	1.001	1.001	24836.675	11648.676
Canada	XBB.1.5.31	0.982	0.957	1.006	1.000	25229.769	12823.027
Canada	XBB.1.5.47	0.979	0.955	1.002	1.000	25909.971	11770.983
Canada	XBB.1.5.32	0.977	0.965	0.988	1.000	26107.411	12173.604
Canada	XBB.1.5.7	0.976	0.956	0.996	1.000	25225.149	12498.934
Canada	XBB.1.5.20	0.970	0.953	0.988	1.000	27428.240	12096.116
Canada	FT.1	0.945	0.925	0.965	1.000	26792.440	11491.241
Canada	XBB.1.5.69	0.934	0.904	0.963	1.000	25785.623	12281.238
Canada	BQ.1.1	0.857	0.822	0.889	1.000	28919.825	12538.675
China	EG.5.1	1.198	1.182	1.214	1.001	3394.461	6749.947
China	FU.1	1.112	1.099	1.124	1.001	2866.909	5047.291
China	FY.3	1.107	1.092	1.123	1.001	3766.592	7191.155
China	XBB.1.16.2	1.106	1.085	1.127	1.001	5505.439	9232.494
China	FR.1.1	1.105	1.087	1.122	1.001	4762.218	8375.087
China	FL.16	1.097	1.077	1.116	1.001	5251.397	8838.607
China	XBB.1.42	1.096	1.073	1.118	1.001	6113.867	10367.651
China	FY.3.1	1.096	1.080	1.112	1.001	4022.764	8396.949
China	XBB.2.3.2	1.089	1.056	1.123	1.000	9933.624	11902.980
China	FE.1.1	1.087	1.067	1.108	1.001	6257.855	8976.966
China	EG.2	1.085	1.059	1.111	1.000	7397.494	10101.266
China	FR.1.3	1.081	1.052	1.110	1.000	9120.002	10638.645
China	GF.1	1.074	1.058	1.090	1.001	4047.622	7973.134

China	FL.4	1.071	1.058	1.084	1.001	3208.886	5673.191
China	XBB.1.16	1.064	1.052	1.077	1.001	3016.906	5799.148
China	XBB.1.16.1	1.063	1.043	1.083	1.000	5912.777	9298.074
China	FL.2.3	1.060	1.046	1.074	1.001	3452.619	6923.746
China	XBB.1.9.1	1.058	1.044	1.072	1.001	3769.872	7041.165
China	XBB.1.5.15	1.051	1.025	1.076	1.001	7875.051	10508.907
China	FL.2	1.048	1.034	1.062	1.001	3892.654	7507.503
China	FL.13	1.046	1.012	1.081	1.000	10088.378	10666.178
China	FL.5	1.037	1.013	1.061	1.000	7368.311	10809.312
China	GR.1	1.036	1.000	1.072	1.000	10610.031	11941.475
China	FL.13.1	1.030	1.008	1.051	1.001	6230.363	9594.446
China	XBB.1.9.2	1.026	1.003	1.051	1.001	7180.414	9327.159
China	XBB.1.5.24	1.023	0.991	1.056	1.000	9366.787	11048.381
China	XBB.1.44.1	1.013	0.982	1.043	1.000	10452.977	11376.953
China	EG.4	1.001	0.970	1.032	1.000	10817.353	12100.357
China	FR.1	0.986	0.954	1.018	1.000	9206.885	11015.016
China	BN.1.2	0.985	0.951	1.019	1.001	11669.478	11050.626
China	FL.4.2	0.982	0.951	1.012	1.000	10452.629	12414.800
China	XBB.1.19.1	0.928	0.905	0.952	1.000	7664.880	10294.506
China	BF.7.14.5	0.824	0.785	0.862	1.000	12552.157	12083.006
China	DY.1	0.819	0.791	0.846	1.000	11315.141	11851.783
China	BF.7.14.1	0.810	0.774	0.847	1.000	13021.484	12119.375
China	DY.2	0.799	0.782	0.816	1.001	6947.947	10625.961
China	DY.4	0.795	0.771	0.820	1.000	11117.544	12424.806
China	BF.7.14	0.792	0.777	0.808	1.001	6442.040	9737.975
China	BA.5.2.48	0.785	0.759	0.810	1.000	10194.251	11262.329
Japan	XBB.1.5.5	1.185	1.149	1.224	1.000	20979.776	11252.480
Japan	EG.5.1	1.154	1.127	1.183	1.000	16970.482	12000.980
Japan	FK.1.3	1.092	1.063	1.121	1.000	19113.664	12266.279
Japan	XBB.1.16.2	1.074	1.054	1.094	1.000	14570.489	11481.217
Japan	XBB.2.3.2	1.060	1.042	1.078	1.000	13226.523	11112.051
Japan	EG.1	1.057	1.040	1.074	1.000	11895.541	11387.662
Japan	FL.4	1.056	1.042	1.071	1.000	10846.646	11131.328
Japan	FU.1	1.054	1.029	1.079	1.000	16282.693	11357.217
Japan	XBB.1.16	1.052	1.041	1.063	1.000	7094.965	9648.008
Japan	EG.2	1.050	1.024	1.076	1.000	17794.055	12395.230
Japan	CJ.1.3	1.041	1.013	1.071	1.000	19324.697	12612.005
Japan	XBB.2.3	1.036	1.013	1.059	1.000	16691.648	12163.123
Japan	XBB.1.16.1	1.035	1.022	1.049	1.000	10098.495	11788.071
Japan	XBB.1.9.2	1.034	1.013	1.055	1.000	14843.659	11463.308
Japan	FL.5	1.031	1.010	1.053	1.000	15482.051	11078.203
Japan	XBB.1.9.1	1.015	1.002	1.028	1.000	8649.161	10967.809
Japan	FL.2	1.004	0.986	1.023	1.001	14069.411	11517.641
Japan	XBB.1.5.24	1.002	0.976	1.026	1.000	19750.344	12504.687
Japan	GR.1	0.996	0.969	1.023	1.001	18199.213	11259.637
Japan	FD.3	0.996	0.961	1.029	1.000	22137.245	12226.277
Japan	EG.4	0.989	0.956	1.021	1.000	21166.280	12451.982
Japan	FR.1	0.983	0.956	1.010	1.000	19909.113	12160.149
Japan	CK.1.1	0.970	0.933	1.007	1.000	21290.210	10780.000
Japan	XBB.1.5.1	0.959	0.926	0.991	1.000	20518.867	12622.277
Japan	BN.1.2	0.955	0.927	0.983	1.000	19839.424	12244.441
Japan	BF.7.15	0.951	0.931	0.970	1.000	15615.758	12124.496
Japan	BQ.1.1.76	0.945	0.906	0.982	1.000	22460.318	12007.958
Japan	BQ.1.1.45	0.928	0.884	0.970	1.001	24045.347	12339.500
Japan	BF.7.4.1	0.927	0.896	0.957	1.001	21116.280	11736.014
Japan	BN.1.3.2	0.921	0.880	0.960	1.000	23324.227	11999.601
Japan	BF.11	0.917	0.876	0.955	1.001	24269.762	12790.234
Japan	BQ.1.1	0.903	0.872	0.933	1.000	21117.241	11793.493
Japan	BN.1.3	0.889	0.844	0.932	1.000	25142.002	11362.317
Japan	XBB.1.5.23	0.889	0.842	0.933	1.000	23604.501	12450.849
Singapore	EG.5.1	1.235	1.180	1.297	1.000	8132.463	9007.638

Singapore	XBB.2.3.11	1.059	1.036	1.084	1.001	5005.086	8520.465
Singapore	FU.1	1.058	1.039	1.077	1.000	3509.181	6040.722
Singapore	XBB.1.16.2	1.048	1.027	1.070	1.000	4189.416	6994.983
Singapore	EG.2	1.040	1.018	1.063	1.000	4365.164	6979.150
Singapore	XBB.1.16.1	1.032	1.017	1.048	1.001	2775.862	5366.814
Singapore	XBB.1.16	1.027	1.012	1.043	1.001	2861.123	5464.513
Singapore	XBB.2.3.2	1.020	1.005	1.035	1.001	2804.818	5384.690
Singapore	FL.4	1.013	0.995	1.031	1.000	3291.625	6193.186
Singapore	XBB.1.16.7	0.995	0.970	1.021	1.000	5638.694	9200.828
Singapore	XBB.2.3	0.993	0.967	1.018	1.000	5444.831	8987.494
Singapore	XBB.1.9.2	0.985	0.964	1.005	1.000	4659.137	8341.666
Singapore	XBB.1.9.1	0.983	0.963	1.003	1.000	4261.377	7804.220
Singapore	XBB.2.3.6	0.983	0.965	1.000	1.001	3693.712	6641.019
Singapore	XBB.1.22.2	0.981	0.955	1.007	1.000	5908.600	9171.395
Singapore	FP.1	0.962	0.941	0.984	1.000	5181.022	8653.313
South Korea	GJ.1	1.204	1.157	1.254	1.001	26821.178	11252.485
South Korea	EG.5.1	1.187	1.165	1.210	1.000	22425.723	11541.056
South Korea	FU.1	1.160	1.130	1.192	1.000	25344.324	10380.414
South Korea	FL.15	1.142	1.111	1.175	1.001	27156.528	11454.385
South Korea	FL.10.1	1.132	1.111	1.154	1.000	22807.406	11980.816
South Korea	XBB.2.3.8	1.102	1.092	1.113	1.000	14007.153	12165.577
South Korea	FL.14	1.099	1.069	1.131	1.000	26322.893	11281.279
South Korea	EG.5.2	1.097	1.066	1.128	1.000	25550.185	10861.972
South Korea	FK.1.1	1.095	1.074	1.118	1.000	21555.860	11470.359
South Korea	EG.2	1.095	1.064	1.127	1.001	24973.929	10184.185
South Korea	XBB.2.3.2	1.095	1.077	1.113	1.000	21059.013	11593.645
South Korea	XBB.1.16.2	1.092	1.078	1.107	1.001	19951.152	11903.790
South Korea	EG.1.4	1.090	1.073	1.107	1.000	20969.523	11093.139
South Korea	FL.2	1.087	1.069	1.105	1.000	18725.661	11577.360
South Korea	XBB.1.16	1.083	1.074	1.091	1.000	12323.214	12067.968
South Korea	FE.1.1	1.082	1.057	1.108	1.000	23801.663	11309.631
South Korea	FL.7	1.074	1.046	1.102	1.000	27402.526	11896.497
South Korea	XBB.2.3.6	1.073	1.045	1.102	1.000	24792.121	11770.817
South Korea	XBB.2.3	1.072	1.056	1.087	1.000	19115.849	12182.297
South Korea	FL.1.2	1.068	1.043	1.094	1.000	24303.272	12505.709
South Korea	XBB.1.16.1	1.065	1.051	1.079	1.000	19027.002	12664.928
South Korea	XBB.1.16.10	1.063	1.046	1.080	1.001	20740.307	11781.284
South Korea	EG.1	1.061	1.053	1.068	1.000	10849.565	12003.285
South Korea	FL.2.1	1.054	1.032	1.077	1.000	24379.259	11720.984
South Korea	FL.1.3	1.053	1.038	1.069	1.000	19844.171	12602.915
South Korea	FL.4	1.052	1.041	1.063	1.000	15237.541	11733.625
South Korea	XBB.1.9.2	1.050	1.041	1.060	1.000	13088.159	12901.111
South Korea	XBB.1.9.1	1.049	1.042	1.057	1.000	11021.529	11977.921
South Korea	EG.4	1.045	1.019	1.072	1.000	25359.738	11982.837
South Korea	XBB.1.5.49	1.041	1.016	1.067	1.001	24713.560	11558.151
South Korea	GR.1	1.041	1.024	1.058	1.000	22610.673	13021.821
South Korea	FL.5	1.040	1.021	1.059	1.000	20444.998	12604.697
South Korea	FL.17.1	1.017	0.990	1.045	1.000	24638.318	11459.372
South Korea	XBB.1.5.23	1.009	0.988	1.030	1.000	21815.671	12427.124
South Korea	FL.13	1.007	0.985	1.028	1.000	24414.314	11964.621
South Korea	FP.4	1.004	0.979	1.028	1.001	22520.137	12601.265
South Korea	XBB.1.5.24	0.999	0.979	1.020	1.000	23463.246	12181.593
South Korea	XBB.1.5.64	0.999	0.976	1.022	1.000	22986.751	12435.895
South Korea	XBB.1.5.17	0.977	0.959	0.996	1.000	23898.131	12323.604
South Korea	BN.1.2.2	0.972	0.946	0.999	1.000	23930.357	11804.581
South Korea	BN.1.2.3	0.941	0.916	0.966	1.001	26065.860	11405.366
South Korea	BQ.1.24	0.936	0.915	0.956	1.000	25220.749	12631.096
South Korea	CH.1.1	0.931	0.913	0.949	1.000	23012.674	12195.537
South Korea	CJ.1.3	0.928	0.914	0.942	1.001	21110.705	12443.726
South Korea	BN.1.3	0.920	0.904	0.936	1.000	21246.728	12592.619
South Korea	BN.1.2	0.913	0.897	0.929	1.000	22503.566	12255.534

South Korea	BN.1.3.5	0.908	0.873	0.941	1.000	28259.078	12208.469
South Korea	BN.1.2.5	0.901	0.879	0.923	1.000	25348.568	12621.264
South Korea	FR.2	0.875	0.844	0.905	1.001	25956.062	12361.490
USA	XBB.1.16.6	1.201	1.175	1.228	1.000	16410.712	12536.031
USA	EG.5.1	1.196	1.179	1.214	1.001	18918.558	12329.176
USA	GJ.1	1.194	1.169	1.220	1.001	17013.484	11778.098
USA	EG.6.1	1.169	1.136	1.203	1.000	16673.797	11531.235
USA	FD.1.1	1.161	1.131	1.193	1.000	18345.408	11955.003
USA	XBB.1.5.72	1.159	1.135	1.184	1.001	18211.762	11834.063
USA	EG.5.2	1.129	1.110	1.149	1.000	18136.499	11953.533
USA	FU.2	1.128	1.101	1.155	1.001	18605.981	11313.770
USA	FY.2	1.121	1.093	1.151	1.000	19137.312	11230.735
USA	FU.1	1.120	1.105	1.134	1.001	18484.296	11676.712
USA	FE.1.1	1.117	1.091	1.144	1.000	17348.747	12275.666
USA	XBB.2.3.2	1.113	1.100	1.127	1.000	18213.638	12405.565
USA	XBB.2.3.3	1.109	1.089	1.130	1.001	17532.282	12311.823
USA	XBB.1.16.2	1.108	1.095	1.122	1.000	18615.970	12800.675
USA	XBB.1.16.1	1.100	1.092	1.108	1.000	16267.451	12673.873
USA	EG.1	1.097	1.086	1.109	1.000	17459.058	11702.997
USA	GR.1	1.097	1.071	1.123	1.000	19651.901	11892.997
USA	XBB.2.3	1.096	1.085	1.107	1.000	18266.846	12320.105
USA	XBB.1.22	1.093	1.072	1.115	1.000	17460.540	12538.347
USA	XBB.1.5.77	1.092	1.075	1.108	1.000	16383.505	12288.488
USA	EG.2	1.089	1.062	1.117	1.000	18241.409	12223.474
USA	XBB.1.16	1.088	1.082	1.093	1.001	14473.584	12779.955
USA	XBB.1.5.44	1.084	1.061	1.107	1.000	17642.435	11739.137
USA	XBB.1.5.59	1.084	1.057	1.111	1.000	18699.869	12152.325
USA	XBB.1.5.28	1.082	1.067	1.097	1.000	18618.327	12022.392
USA	FL.4	1.081	1.070	1.092	1.001	17930.002	12133.524
USA	FE.1.2	1.080	1.060	1.101	1.000	18770.429	11970.842
USA	FL.3	1.080	1.056	1.104	1.000	20246.380	12678.376
USA	XBB.1.5.68	1.077	1.062	1.092	1.000	19759.163	12580.766
USA	XBB.1.5.37	1.075	1.058	1.093	1.000	18145.562	12607.805
USA	EU.1.1	1.074	1.057	1.090	1.000	18444.647	12263.702
USA	EG.1.4	1.072	1.048	1.097	1.000	19430.973	12725.575
USA	XBB.1.5.10	1.065	1.054	1.076	1.000	16379.942	12538.586
USA	XBB.1.5.39	1.063	1.036	1.091	1.001	18204.317	12804.718
USA	FL.2	1.062	1.048	1.076	1.000	16842.660	12681.152
USA	XBB.1.9.1	1.062	1.055	1.069	1.000	18235.379	13280.757
USA	FL.13	1.057	1.032	1.082	1.000	18943.728	12995.630
USA	XBB.1.5.86	1.055	1.029	1.080	1.000	18968.214	12150.805
USA	XBB.1.5.73	1.054	1.034	1.073	1.000	18520.659	13017.283
USA	FL.5	1.049	1.032	1.066	1.000	18018.316	12742.318
USA	XBB.1.9.2	1.041	1.030	1.051	1.000	17988.209	12412.351
USA	XBB.1.19.1	1.033	1.009	1.057	1.000	18484.396	12887.096
USA	XBB.1.17.1	1.033	1.005	1.061	1.000	18716.936	12167.809
USA	XBB.1.5.18	1.032	1.003	1.061	1.000	17260.252	12056.514
USA	XBB.1.5.56	1.031	1.004	1.058	1.000	18807.117	12600.717
USA	XBB.1.5.12	1.030	1.005	1.054	1.000	17995.093	12958.361
USA	XBB.1.5.80	1.029	1.002	1.055	1.000	16127.215	13053.516
USA	XBB.1.5.30	1.025	1.007	1.043	1.000	17869.061	11544.140
USA	XBB.1.5.27	1.024	1.003	1.046	1.000	19764.876	12810.216
USA	EG.4	1.024	1.005	1.044	1.000	17505.779	11955.009
USA	XBB.1.5.48	1.024	1.007	1.041	1.000	17092.683	12631.377
USA	XBB.1.5.50	1.024	0.997	1.050	1.000	19099.514	12640.215
USA	FL.12	1.023	0.994	1.051	1.001	19924.466	12717.493
USA	XBB.1.5.49	1.020	1.013	1.028	1.000	18260.512	12379.533
USA	XBB.1.5.1	1.020	1.010	1.029	1.000	18389.446	12267.234
USA	XBB.1.5.24	1.019	0.997	1.041	1.000	19023.282	13218.202
USA	XBB.1.5.4	1.018	1.004	1.031	1.000	18461.555	12655.774
USA	FL.10	1.018	0.992	1.043	1.000	18792.308	12915.634

USA	XBB.1.5.3	1.012	0.986	1.038	1.000	19810.276	12893.577
USA	XBB.1.5.35	1.012	0.998	1.026	1.000	18355.999	12100.719
USA	XBB.1.5.17	1.011	0.999	1.023	1.000	17662.708	12242.314
USA	XBB.1.5.61	1.008	0.980	1.035	1.001	19314.606	13238.328
USA	XBB.1.5.16	1.006	0.987	1.025	1.000	19011.037	12860.989
USA	XBB.1.5.20	1.005	0.988	1.022	1.000	19191.794	12571.352
USA	XBB.1.5.31	1.004	0.983	1.025	1.000	19544.483	13065.938
USA	XBB.1.5.14	1.004	0.975	1.031	1.000	19798.408	11947.783
USA	XBB.1.5.15	1.002	0.991	1.013	1.000	18082.609	12591.057
USA	FD.4	1.002	0.982	1.021	1.000	18758.790	12412.018
USA	XBB.1.5.7	1.001	0.980	1.022	1.000	20528.201	12445.128
USA	XBB.1.5.51	1.001	0.984	1.018	1.000	17757.650	14099.442
USA	XBB.1.5.78	1.001	0.977	1.024	1.000	19564.041	13006.153
USA	EK.2	1.000	0.969	1.030	1.000	19820.082	13051.270
USA	CH.1.1	0.995	0.962	1.026	1.000	18244.659	13174.267
USA	XBB.1.5.9	0.992	0.959	1.026	1.000	19099.569	12765.173
USA	XBB.1.5.62	0.991	0.962	1.019	1.000	17983.481	12270.645
USA	XBB.1.5.41	0.987	0.955	1.017	1.000	15573.811	12338.776
USA	XBB.1.5.2	0.986	0.966	1.007	1.000	18766.951	11257.246
USA	XBB.1.5.13	0.986	0.974	0.998	1.000	18391.317	12406.034
USA	XBB.1.5.32	0.982	0.966	0.998	1.000	19360.960	13101.399
USA	XBB.1.5.52	0.981	0.961	1.001	1.000	19273.741	13174.876
USA	XBB.1.5.66	0.978	0.957	0.998	1.000	18534.671	13452.254
USA	XBB.1.5.21	0.976	0.956	0.996	1.000	18110.950	12721.728
USA	XBB.1.5.11	0.974	0.950	0.998	1.000	17570.825	13098.179
USA	BQ.1.1	0.968	0.942	0.993	1.000	19096.719	12964.322
USA	XBB.1.5.69	0.961	0.938	0.984	1.000	20636.413	12125.611
USA	FD.2	0.957	0.943	0.970	1.000	20007.236	13440.453
USA	XBB.1.5.33	0.947	0.926	0.967	1.000	19811.713	13486.054
USA	XBB.1.5.19	0.947	0.916	0.976	1.000	17703.735	13347.167
USA	XBB.1.5.5	0.936	0.899	0.970	1.000	17211.557	13037.697

The Re value of XBB.1.5 is set at 1.

Table S3. Primers used in this study

Primer name	Primer sequence (5'-to-3')	Purpose
Omicron universal Fw	cactatagggcgaattgggtaccatgtttgtgttcctggt	Preparation of S expression plasmid
BA.2 WT Rv	agctccaccgcggtggcggccgctcaggtgtagtgcagtttca	Preparation of S expression plasmid
XBB.1.5_F456L_Fw	ctacctctacagactgCTGaggaagagcaagctg	Preparation of S expression plasmid
XBB.1.5_F456L_Rv	cagcttgctcttcctCAGcagtctgtagaggtag	Preparation of S expression plasmid
XBB.1.5_Q52H_Fw	gtgctgcacagcaccCACgacctgttcctgcc	Preparation of S expression plasmid
XBB.1.5_Q52H_Rv	ggcaggaacaggtcGTGggtgctgtgcagcac	Preparation of S expression plasmid

Supplementary figure

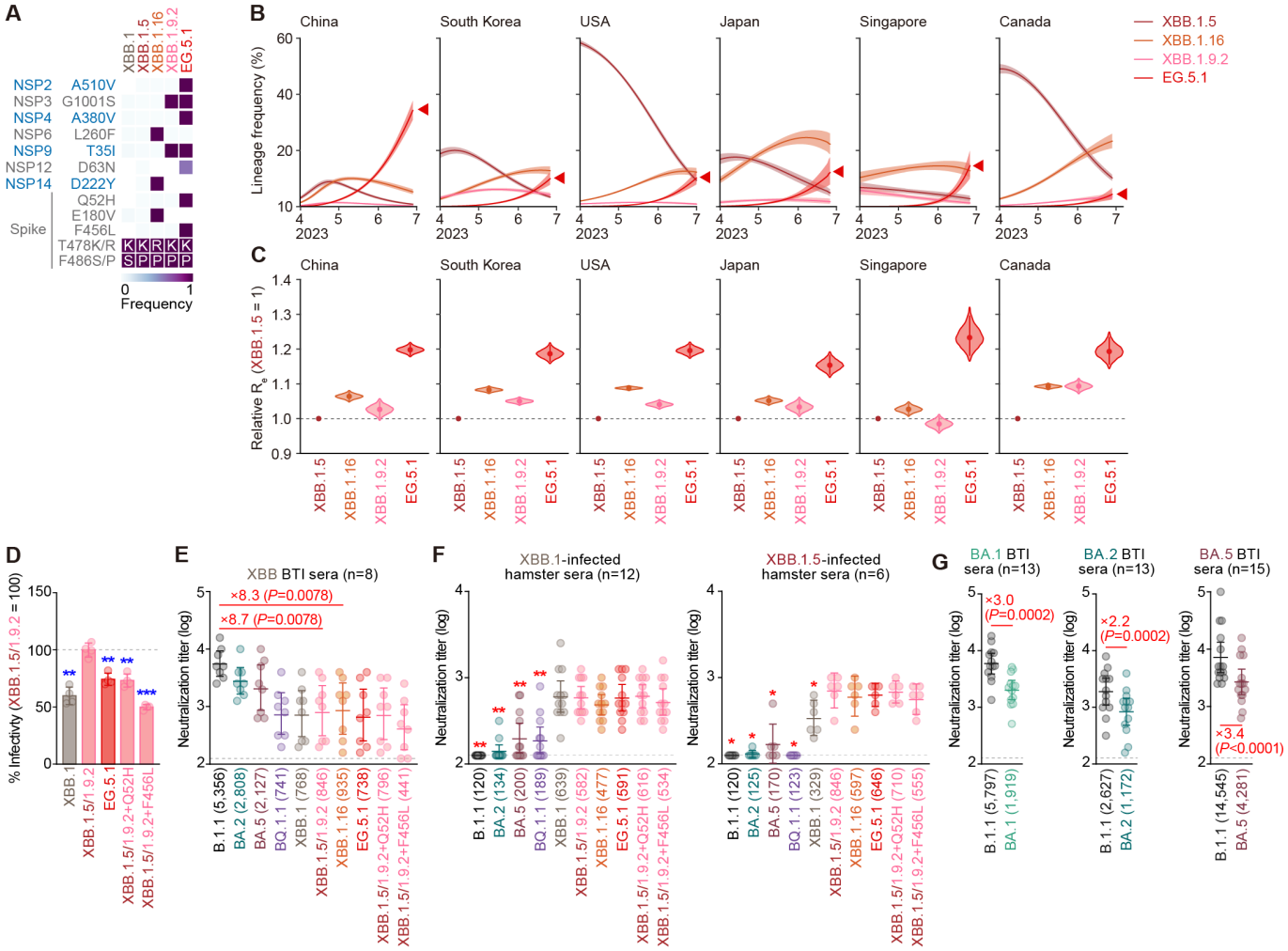

Figure S1. Virological features of EG.5.1 and XBB BTI

(**A**) Frequency of mutations of interest in the representative XBB sublineages. Only mutations with a frequency >0.5 in at least one but not all the representative sublineages are shown. Note that the S proteins of XBB.1.5 and XBB.1.9.2 are identical.

(**B**) Estimated epidemic dynamics of the representative XBB sublineages in countries where >50 sequences of EG.5.1, XBB.1.5, XBB.1.9.2, and XBB.1.16 were detected from April 1, 2023 to July 13, 2023. Countries are ordered according to the number of detected sequences of EG.5.1. Line, posterior mean; ribbon, 95% Bayesian confidence interval. The dynamics for EG.5.1 is highlighted by a red arrowhead.

(**C**) Estimated relative R_e of the representative XBB sublineages in the six countries. The relative R_e of XBB.1.5 is set to 1 (horizontal dashed line). Violin, posterior distribution; dot, posterior mean; line, 95% Bayesian confidence interval.

(**D**) Lentivirus-based pseudovirus assay. HOS-ACE2-TMPRSS2 cells were infected with pseudoviruses bearing each S protein. The amount of input virus was normalized to the amount of HIV-1 p24 capsid protein. The percentage infectivity of XBB.1.5/1.9.2, XBB.1.5/1.9.2+Q52H, XBB.1.5/1.9.2+F456L, and EG.5.1 compared to that of XBB.1.5/1.9.2 are shown. The horizontal

dash line indicates the mean value of the percentage infectivity of the XBB.1.5/1.9.2. Assays were performed in quadruplicate. The presented data are expressed as the average ± SD. Each dot indicates the result of an individual replicate.

(**E-G**) Neutralization assay. Assays were performed with pseudoviruses harboring the S proteins of B.1.1, BA.1, BA.2, BA.5, BQ.1.1, XBB.1, XBB.1.5/1.9.2, XBB.1.16, EG.5.1, XBB.1.5/1.9.2+Q52H, and XBB.1.5/1.9.2+F456L. The following sera were used: convalescent sera from fully vaccinated individuals who had been infected with XBB.1.5 (one 3-dose vaccinated. 1 donor in total), XBB.1.9 (one 3-dose vaccinated donor, one 4-dose vaccinated donor and one 5-dose vaccinated donor. 3 donors in total), and XBB.1.16 (one 2-dose vaccinated donor, two 3-dose vaccinated donors, and one 4-dose vaccinated donor. 4 donors in total) (**E**); sera from hamster infected with XBB.1 (left) or XBB.1.5 (right) (**F**); and convalescent sera from fully vaccinated individuals who had been infected with BA.1 (thirteen 2-dose vaccinated, 13 donors in total) (left)[1], BA.2 (nine 2-dose vaccinated and four 3-dose vaccinated donors. 13 donors in total) (middle)[19], and BA.5 (one 2-dose vaccinated, thirteen 3-dose vaccinated donors, and one 4-dose vaccinated. 15 donors in total) (right)[19] (**G**). Each dot indicates the result of an individual replicate. Assays for each serum sample were performed in triplicate to determine the 50% neutralization titer (NT_{50}). Each dot represents one NT_{50} value, and the geometric mean and 95% confidence interval are shown. The number in parenthesis indicates the mean of NT_{50} values. The horizontal dash line indicates the detection limit (120-fold).

In **D**, statistically significant differences (**, $P < 0.001$, ***, $P < 0.0001$) versus XBB.1.5/1.9.2 were determined by two-sided Student's *t* tests. Blue asterisks indicate decreased percentage of infectivity.

In **E and G**, statistically significant differences versus B.1.1 were determined by two-sided Wilcoxon signed-rank tests. The fold change between B.1.1 and the variant indicated is shown in red. Background information on the convalescent donors is summarized in **Table S1.**

In **F**, statistically significant differences (*, $P < 0.01$, **, $P < 0.001$) between B.1.1 and XBB.1 (left) or XBB.1.5/1.9.2 (right) were determined by two-sided Wilcoxon signed-rank tests and indicated with asterisks. Red asterisks indicate decreased NT_{50}s.

Consortia

The Genotype to Phenotype Japan (G2P-Japan) Consortium

The Institute of Medical Science, The University of Tokyo, Japan
Naoko Misawa, Ziyi Guo, Alfredo A. Hinay Jr., Arnon Plianchaisuk, Jarel Elgin M. Tolentino, Luo Chen, Shigeru Fujita, Lin Pan, Gustav Joas, Olivia Putri, Yoonjin Kim, Mai Suganami, Mika Chiba, Ryo Yoshimura, Kyoko Yasuda, Keiko Iida, Naomi Ohsumi, Adam P. Strange, Shiho Tanaka

Hokkaido University, Japan
Takasuke Fukuhara, Tomokazu Tamura, Rigel Suzuki, Saori Suzuki, Hayato Ito, Keita Matsuno, Hirofumi Sawa, Naganori Nao, Shinya Tanaka, Masumi Tsuda, Lei Wang, Yoshikata Oda, Zannatul Ferdous, Kenji Shishido

Tokai University, Japan
So Nakagawa

Kyoto University, Japan
Kotaro Shirakawa, Akifumi Takaori-Kondo, Kayoko Nagata, Ryosuke Nomura, Yoshihito Horisawa, Yusuke Tashiro, Yugo Kawai, Kazuo Takayama, Rina Hashimoto, Sayaka Deguchi, Yukio Watanabe, Ayaka Sakamoto, Naoko Yasuhara, Takao Hashiguchi, Tateki Suzuki, Kanako Kimura, Jiei Sasaki, Yukari Nakajima, Hisano Yajima

Hiroshima University, Japan
Takashi Irie, Ryoko Kawabata

Kyushu University, Japan
Kaori Tabata

Kumamoto University, Japan
Terumasa Ikeda, Hesham Nasser, Ryo Shimizu, MST Monira Begum, Michael Jonathan, Yuka Mugita, Otowa Takahashi, Kimiko Ichihara, Takamasa Ueno, Chihiro Motozono, Mako Toyoda

University of Miyazaki, Japan
Akatsuki Saito, Maya Shofa, Yuki Shibatani, Tomoko Nishiuchi

Acknowledgments

We would like to thank all members of The Genotype to Phenotype Japan (G2P-Japan) Consortium. We thank Dr. Kenzo Tokunaga (National Institute of Infectious Diseases, Japan) for sharing materials. We gratefully acknowledge the numerous laboratories worldwide that have provided sequence data and metadata to GISAID. A full list of originating and submitting laboratories for the sequences used in our analysis can be found at https://www.gisaid.org using the EPI-SET-ID: EPI_SET_230725pv.

Supplementary References

1. Yamasoba D, Kimura I, Nasser H, et al. Virological characteristics of the SARS-CoV-2 Omicron BA.2 spike. *Cell* 2022; **185**(12): 2103-15.e19.
2. Kimura I, Yamasoba D, Tamura T, et al. Virological characteristics of the novel SARS-CoV-2 Omicron variants including BA.4 and BA.5. *Cell* 2022; **185**(21): 3992-4007.e16.
3. Saito A, Tamura T, Zahradnik J, et al. Virological characteristics of the SARS-CoV-2 Omicron BA.2.75 variant. *Cell Host Microbe* 2022; **30**(11): 1540–55.e15.
4. Tamura T, Ito J, Uriu K, et al. Virological characteristics of the SARS-CoV-2 XBB variant derived from recombination of two Omicron subvariants. *Nat Commun* 2023; **14**(1): 2800.
5. Uriu K, Kimura I, Shirakawa K, et al. Neutralization of the SARS-CoV-2 Mu variant by convalescent and vaccine serum. *N Engl J Med* 2021; **385**(25): 2397-9.
6. Fujita S, Kosugi Y, Kimura I, Yamasoba D, The Genotype to Phenotype Japan (G2P-Japan) Consortium, Sato K. Structural Insight into the Resistance of the SARS-CoV-2 Omicron BA.4 and BA.5 Variants to Cilgavimab. *Viruses* 2022; **14**(12): 2677.
7. Ferreira I, Kemp SA, Datir R, et al. SARS-CoV-2 B.1.617 mutations L452R and E484Q are not synergistic for antibody evasion. *J Infect Dis* 2021; **224**(6): 989-94.
8. Uriu K, Cardenas P, Munoz E, et al. Characterization of the immune resistance of SARS-CoV-2 Mu variant and the robust immunity induced by Mu infection. *J Infect Dis* 2022.
9. Kimura I, Kosugi Y, Wu J, et al. The SARS-CoV-2 Lambda variant exhibits enhanced infectivity and immune resistance. *Cell Rep* 2022; **38**(2): 110218.
10. Saito A, Irie T, Suzuki R, et al. Enhanced fusogenicity and pathogenicity of SARS-CoV-2 Delta P681R mutation. *Nature* 2022; **602**(7896): 300-6.
11. Yamasoba D, Kosugi Y, Kimura I, et al. Neutralisation sensitivity of SARS-CoV-2 omicron subvariants to therapeutic monoclonal antibodies. *Lancet Infect Dis* 2022; **22**(7): 942-3.
12. Ito J, Suzuki R, Uriu K, et al. Convergent evolution of the SARS-CoV-2 Omicron subvariants leading to the emergence of BQ.1.1 variant. *BioRxiv* 2022: doi: https://doi.org/10.1101/2022.12.05.519085.
13. Kimura I, Yamasoba D, Nasser H, et al. The SARS-CoV-2 spike S375F mutation characterizes the Omicron BA.1 variant. *iScience* 2022; **25**(12): 105720.
14. Tamura T, Ito J, Uriu K, et al. Virological characteristics of the SARS-CoV-2 XBB variant derived from recombination of two Omicron subvariants. *BioRxiv* 2022: doi: https://doi.org/10.1101/2022.12.27.521986.
15. Motozono C, Toyoda M, Zahradnik J, et al. SARS-CoV-2 spike L452R variant evades cellular immunity and increases infectivity. *Cell Host Microbe* 2021; **29**(7): 1124-36.
16. Meng B, Abdullahi A, Ferreira IATM, et al. Altered TMPRSS2 usage by SARS-CoV-2 Omicron impacts tropism and fusogenicity. *Nature* 2022; **603**(7902): 706-14.
17. Ito J, Suzuki R, Uriu K, et al. Convergent evolution of the SARS-CoV-2 Omicron subvariants leading to the emergence of BQ.1.1 variant. *Nat Commun* 2023; **14**(1): 2671.

18. Uriu K, Ito J, Zahradnik J, et al. Enhanced transmissibility, infectivity, and immune resistance of the SARS-CoV-2 omicron XBB.1.5 variant. *Lancet Infect Dis* 2023; **23**(3): 280-1.
19. Yamasoba D, Uriu K, Plianchaisuk A, et al. Virological characteristics of the SARS-CoV-2 omicron XBB.1.16 variant. *Lancet Infect Dis* 2023; **23**(6): 655-6.
20. Niwa H, Yamamura K, Miyazaki J. Efficient selection for high-expression transfectants with a novel eukaryotic vector. *Gene* 1991; **108**(2): 193-9.
21. Ozono S, Zhang Y, Ode H, et al. SARS-CoV-2 D614G spike mutation increases entry efficiency with enhanced ACE2-binding affinity. *Nat Commun* 2021; **12**(1): 848.
22. Fujita S, Kosugi Y, Kimura I, Yamasoba D, The Genotype to Phenotype Japan (G2P-Japan) Consortium, Sato K. Structural Insight into the Resistance of the SARS-CoV-2 Omicron BA.4 and BA.5 Variants to Cilgavimab. *Viruses* 2022; **14**(12): 2677.
23. Ozono S, Zhang Y, Tobiume M, Kishigami S, Tokunaga K. Super-rapid quantitation of the production of HIV-1 harboring a luminescent peptide tag. *J Biol Chem* 2020; **295**(37): 13023-30.